

ISOLATION AND STRUCTURAL STUDIES OF PHOSPHATE-CONTAINING OLIGOSACCHARIDES FROM ALKALINE AND ACID HYDROLYSATES OF *Streptococcus pneumoniae* TYPE 6^B CAPSULAR POLYSACCHARIDE

JAN E. G. VAN DAM, JAN BREG, RONALD KOMEN, JOHANNIS P. KAMERLING, AND JOHANNES F. G. VLIEGENTHART

Department of Bio-Organic Chemistry, Transitorium III, Utrecht University, P.O. Box 80.075, NL-3508 TB Utrecht (The Netherlands)

(Received July 7th, 1988; accepted for publication, November 12th, 1988)

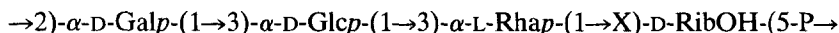
ABSTRACT

The capsular polysaccharide of *Streptococcus pneumoniae* serotype 6^B $[\rightarrow 2)\text{-}\alpha\text{-D-Galp-(1}\rightarrow 3)\text{-}\alpha\text{-D-Glcp-(1}\rightarrow 3)\text{-}\alpha\text{-L-Rhap-(1}\rightarrow 4)\text{-D-RibOH-(5-P}\rightarrow]_n$ was depolymerised under alkaline (NaOH) and acidic (HF) conditions. The former treatment yielded, as the major component, $\alpha\text{-2-P-Galp-(1}\rightarrow 3)\text{-}\alpha\text{-Glcp-(1}\rightarrow 3)\text{-}\alpha\text{-Rhap-(1}\rightarrow 4)\text{-5-P-RibOH}$. The latter treatment at -16° gave $\alpha\text{-Galp-(1}\rightarrow 3)\text{-}\alpha\text{-Glcp-(1}\rightarrow 3)\text{-}\alpha\text{-Rhap-(1}\rightarrow 4)\text{-RibOH-(5-P}\rightarrow 2)\text{-}\alpha\text{-Galp-(1}\rightarrow 3)\text{-}\alpha\text{-Glcp-(1}\rightarrow 3)\text{-}\alpha\text{-Rhap-(1}\rightarrow 4)\text{-RibOH}$ and at 4° gave $\alpha\text{-Galp-(1}\rightarrow 3)\text{-}\alpha\text{-Glcp-(1}\rightarrow 3)\text{-}\alpha\text{-Rhap-(1}\rightarrow 4)\text{-RibOH}$. These oligosaccharides were characterised by sugar analysis, f.a.b.-m.s., and $^1\text{H-}$ and $^{13}\text{C-n.m.r.}$ spectroscopy.

INTRODUCTION

In seeking to develop semi-synthetic vaccines to *Streptococcus pneumoniae*, the graded depolymerisation of capsular polysaccharides has been studied in order to obtain oligosaccharide determinants for conjugation to carriers¹ and for immunological inhibition studies.

Pneumococci of group 6 are divided into two cross-reactive types 6^A and 6^B (6 and 26 in the U.S. classification system²). The capsular polysaccharides^{3,4} S6^A (1) and S6^B (2) differ only in the rhamnosyl-ribitol linkages which are (1 \rightarrow 3) for S6^A and (1 \rightarrow 4) for S6^B. The stability of S6^A towards hydrolysis is lower than that of S6^B, since polymers with phosphoric diesters having adjacent hydroxyl groups, such as in S6^A, are gradually degraded in solution⁵. Because the antigenicity and immunogenicity of capsular polysaccharides are related directly to their molecular mass^{6,7}, the expanded polyvalent pneumococcal polysaccharide vaccine^{5,8} Pneumovax[®] 23 contains S6^B.



1 S6^A, X = 3

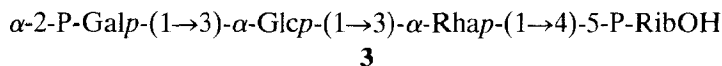
2 S6^B, X = 4

The failure of the pneumococcal polysaccharide vaccines Pneumovax® 14 and 23 to provide protection against specific infections with group 6 pneumococci in infancy prompted an investigation of the possibilities for conjugation to carriers of oligosaccharide-determinants derived from *Streptococcus pneumoniae* group 6 capsular polysaccharides. Chemical and enzymic hydrolysis^{3,4} have been used for the structural analysis of **1** and **2**. Alkaline hydrolysis of **1** yielded phosphoric monoesters in which almost all of the phosphate is attached to RibOH, and treatment with alkaline phosphatase afforded the dephosphorylated tetrasaccharide³. Treatment of **2** with hydrogen fluoride⁴ gave the dephosphorylated tetrasaccharide only. Non-characterised reducing oligosaccharides, derived from **1** by graded acid hydrolysis, when coupled to a protein carrier⁹ showed high immunogenicity with specificity for both the carrier protein and **1**.

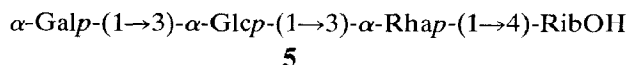
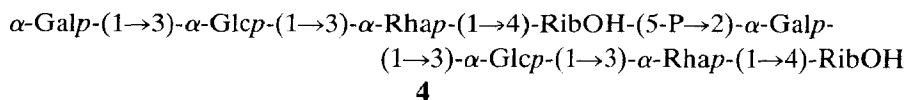
We now describe partial depolymerisation of **2** to yield well-defined oligosaccharides.

RESULTS AND DISCUSSION

Treatment of **2** with 10mM NaOH yielded **3**, a tetrasaccharide with a phosphate group at each end, as a major product.



Hydrolysis of **2** with aqueous 48% HF at 4° for 48 h (method I) gave small quantities of a series of oligosaccharides from which **4** and **5** could be isolated. Treatment of **2** for 4 days at -16° (method II) afforded **4** as the major product, together with two minor oligosaccharides corresponding to higher oligomers of the repeating tetrasaccharide linked *via* phosphoric diester bonds.



Sugar analysis. — The compositions of **3–5** were established *via* g.l.c. of their trimethylsilylated methanolsates. The molar ratios of Gal, Glc, Rha, RibOH, and 2,5-anhydro-RibOH were as follows: **3**, 0.9:1.0:0.9:0.9; **4**, 1.0:1.0:1.0:0.5:0.7; and **5**, 1.0:1.0:1.0:0.8:0.2. As found for the native polysaccharide, phosphorylated RibOH gave only trimethylsilylated 2,5-anhydro-RibOH (R_M 0.38), a phenomenon which has been observed in the analysis of teichoic acids^{10,11}. G.l.c.–m.s. of the anhydro-alditol gave characteristic ions at m/z 350 [M]⁺, 335 [M - CH₃]⁺, 319 [M

$-\text{HOCH}_2^+$, 260 $[\text{M} - \text{HOSiMe}_3]^+$, 247 $[\text{M} - \text{CH}_2\text{OSiMe}_3]^+$, 204 $[(\text{CHOSiMe}_3)_2]^+$, and 170 $[260 - \text{HOSiMe}_3]^+$. For non-phosphorylated RibOH, the major product was trimethylsilylated RibOH.

F.a.b.-m.s. — The negative-ion spectrum of **3** contained a signal for $[\text{M} - \text{H}]^-$ at m/z 781, in accordance with a tetrasaccharide having two terminal monophosphate esters. Cleavage of one phosphate group yielded intense peaks at m/z 701 $\{[(\text{M} - \text{H}) - \text{HPO}_3]^- \}$ and 683 $\{[(\text{M} - \text{H}) - \text{H}_3\text{PO}_4]^- \}$. The fragment ions m/z 567 $\{[(\text{P}-\text{O}-\text{Gal}-\text{O}-\text{Glc}-\text{O}-\text{Rha}-\text{OH}) - \text{H}]^- \}$, 539 $\{[(\text{HO}-\text{Glc}-\text{O}-\text{Rha}-\text{O}-\text{RibOH}-\text{O}-\text{P}) - \text{H}]^- \}$, 421 $\{[(\text{P}-\text{O}-\text{Gal}-\text{O}-\text{Glc}-\text{OH}) - \text{H}]^- \}$, 377 $\{[(\text{HO}-\text{Rha}-\text{O}-\text{RibOH}-\text{O}-\text{P}) - \text{H}]^- \}$, 259 $\{[(\text{P}-\text{O}-\text{Gal}-\text{OH}) - \text{H}]^- \}$, and 231 $\{[(\text{HO}-\text{RibOH}-\text{O}-\text{P}) - \text{H}]^- \}$ correspond to cleavage of glycosidic linkages and can be derived from $[\text{M} - \text{H}]^-$ ions by back rearrangement of hydrogen¹². The fragment ions are accompanied by ions of 2 and 18 a.m.u. lower¹³, corresponding to elimination of H_2 and H_2O , respectively. For fragment ions formed at the anomeric carbon atom, it is also possible that a formyl group is left at the interglycosidic oxygen atom¹², as is evident from a pair of peaks at m/z 377 and 405 $\{[(\text{HOC}-\text{O}-\text{Rha}-\text{O}-\text{RibOH}-\text{O}-\text{P}) - \text{H}]^- \}$. The above-mentioned peaks at m/z 567 and 259 can also be explained as fragments retaining a formyl group, namely, $[(\text{HOC}-\text{O}-\text{Glc}-\text{O}-\text{Rha}-\text{O}-\text{RibOH}-\text{O}-\text{P}) - \text{H}]^-$ and $[(\text{HOC}-\text{O}-\text{RibOH}-\text{O}-\text{P}) - \text{H}]^-$.

The negative-ion spectrum of **4** contained a signal for $[\text{M} - \text{H}]^-$ at m/z 1305 for two tetrasaccharide units linked *via* a phosphoric diester bond. As described for **3**, there was a series of fragment ions at m/z 1171 $\{[(\text{Gal}-\text{O}-\text{Glc}-\text{O}-\text{Rha}-\text{O}-\text{RibOH}-\text{O}-\text{P}-\text{O}-\text{Gal}-\text{O}-\text{Glc}-\text{O}-\text{Rha}-\text{OH}) - \text{H}]^- \}$, 1143 $\{[(\text{HO}-\text{Glc}-\text{O}-\text{Rha}-\text{O}-\text{RibOH}-\text{O}-\text{P}-\text{O}-\text{Gal}-\text{O}-\text{Glc}-\text{O}-\text{Rha}-\text{O}-\text{RibOH}) - \text{H}]^- \}$, 1025 $\{[(\text{Gal}-\text{O}-\text{Glc}-\text{O}-\text{Rha}-\text{O}-\text{RibOH}-\text{O}-\text{P}-\text{O}-\text{Gal}-\text{O}-\text{Glc}-\text{OH}) - \text{H}]^- \}$, 981 $\{[(\text{HO}-\text{Rha}-\text{O}-\text{RibOH}-\text{O}-\text{P}-\text{O}-\text{Gal}-\text{O}-\text{Glc}-\text{O}-\text{Rha}-\text{O}-\text{RibOH}) - \text{H}]^- \}$, 863 $\{[(\text{Gal}-\text{O}-\text{Glc}-\text{O}-\text{Rha}-\text{O}-\text{RibOH}-\text{O}-\text{P}-\text{O}-\text{Gal}-\text{OH}) - \text{H}]^- \}$, 835 $\{[(\text{HO}-\text{RibOH}-\text{O}-\text{P}-\text{O}-\text{Gal}-\text{O}-\text{Glc}-\text{O}-\text{Rha}-\text{O}-\text{RibOH}) - \text{H}]^- \}$, and 701 $\{[(\text{HO}-\text{P}-\text{O}-\text{Gal}-\text{O}-\text{Glc}-\text{O}-\text{Rha}-\text{O}-\text{RibOH}) - \text{H}]^-$ or $\{[(\text{Gal}-\text{O}-\text{Glc}-\text{O}-\text{Rha}-\text{O}-\text{RibOH}-\text{O}-\text{P}-\text{OH}) - \text{H}]^- \}$, due to cleavage of glycosidic bonds. Furthermore, a parallel series of fragment ions can be formed when a formyl group is left at the interglycosidic oxygen atom (see **3**). Thus, the relatively intense fragment at m/z 1009 can be ascribed to $[(\text{HOC}-\text{O}-\text{Rha}-\text{O}-\text{RibOH}-\text{O}-\text{P}-\text{O}-\text{Gal}-\text{O}-\text{Glc}-\text{O}-\text{Rha}-\text{O}-\text{RibOH}) - \text{H}]^-$, whereas the above-mentioned primary sequence peaks at m/z 1171 and 863 can be explained additionally as $[(\text{HOC}-\text{O}-\text{Glc}-\text{O}-\text{Rha}-\text{O}-\text{RibOH}-\text{O}-\text{P}-\text{O}-\text{Gal}-\text{O}-\text{Glc}-\text{O}-\text{Rha}-\text{O}-\text{RibOH}) - \text{H}]^-$ and $[(\text{HOC}-\text{O}-\text{RibOH}-\text{O}-\text{P}-\text{O}-\text{Gal}-\text{O}-\text{Glc}-\text{O}-\text{Rha}-\text{O}-\text{RibOH}) - \text{H}]^-$, respectively. Each of the various fragments discussed contains phosphate, indicating that the fragmentation of the molecule is dictated by the phosphate group.

Positive-ion *f.a.b.-m.s.* of **5** gave a pseudomolecular ion $[\text{M} + \text{H}]^+$ at m/z 623 in accordance with the dephosphorylated tetrasaccharide. In addition, cationised ions at m/z 645 $[\text{M} + \text{Na}]^+$ and 640 $[\text{M} + \text{NH}_4]^+$ were found. Because of interference with background peaks, the sequence ions are not presented.

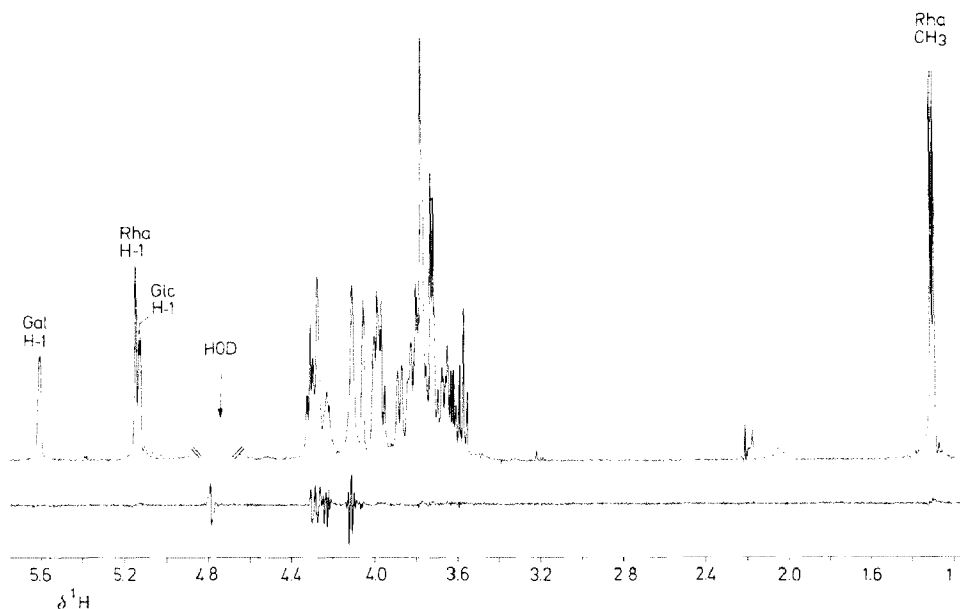


Fig. 1. 500-MHz ^1H -N.m.r. spectrum of **3**. Included is the difference-spectrum with the corresponding ^{31}P -decoupled ^1H -n.m.r. spectrum.

N.m.r. spectroscopy. — (a) *Tetrasaccharide 3*. The 500-MHz ^1H -n.m.r. spectrum of **3** (Fig. 1) contains three signals for anomeric protons, the positions and coupling constants of which accord with α sugars. A doublet at δ 1.308 is observed for CH_3 of Rha and signals for the skeleton protons of all the sugar residues are found at δ 4.35–3.55. The difference-spectrum, obtained after subtracting the corresponding ^{31}P -decoupled 500-MHz ^1H -n.m.r. spectrum, is included in Fig. 1 and indicates three signals each with ^{31}P , ^1H coupling, at δ 4.289, 4.238, and 4.110, respectively, corresponding to Gal H-2, RibOH H-5, and H-5' (Table I). The assignment of these resonances, those of the anomeric protons, and those of most of the skeleton protons is obtained from a ^1H - ^1H COSY spectrum of **3** (Fig. 2).

The signal for Rha H-1 at δ 5.159 is identified by the multiplet for H-2, $J_{2,3}$ for Rha being ~ 3 Hz in contrast to $J_{2,3} \sim 9$ Hz for Glc and Gal. For Rha, all cross-peaks between contiguous protons are clearly discernible in the ^1H - ^1H COSY spectrum, starting with CH_3 or H-1, and indicating chemical shift values for the resonances of all the Rha protons (Table I).

The signal for Gal H-1 is assigned at δ 5.623 on account of the position of the resonance of Gal H-2 at δ 4.289, in accordance with the region of 4.1–4.3 p.p.m. found in the above-mentioned difference-spectrum. This signal is broadened by a $^3J_{\text{POCH}}$ coupling of ~ 8 Hz, as determined from the difference-spectrum in Fig. 1. For Gal, the assignment of the resonances for H-1,2,3,4 is then obtained straightforwardly from the ^1H - ^1H COSY spectrum (Fig. 2). The small value of $J_{4,5}$ yields a low-intensity cross-peak of Gal H-4 with its H-5 at δ 4.329. There is only

TABLE I

¹H-N.M.R. CHEMICAL SHIFT DATA^a (δ) FOR **3** AND **4**, TOGETHER WITH THOSE FOR RIBOH AND THE RESPECTIVE METHYL α -GLYCOPYRANOSIDES OF THE CONSTITUENT MONOSACCHARIDES^b

Proton	Compound				
		3	4		Methyl α -glycopyranosides and RibOH
			Gly'	Gly	
Gal	H-1	5.623	5.399	5.623	4.837
	H-2	4.289	3.838	4.295	3.819
	H-3	4.004	3.911	4.007	3.811
	H-4	4.069	4.015	4.066	3.968
	H-5	4.329	4.259	4.314	3.897
	H-6	3.74	3.728	3.739	3.743
	H-6'	3.74	3.728	3.739	3.749
Glc	H-1	5.141	5.153	5.118	4.806
	H-2	3.672	3.679	3.686	3.558
	H-3	3.978	3.945	3.985	3.664
	H-4	3.719	3.725	3.692	3.398
	H-5	3.993	4.008	3.993	3.664
	H-6	3.79	3.79	3.79	3.868
	H-6'	3.79	3.79	3.79	3.752
Rha	H-1	5.159	5.153	5.077	4.688
	H-2	4.283	4.292	4.259	3.922
	H-3	3.883	3.886	3.893	3.703
	H-4	3.579	3.580	3.588	3.430
	H-5	3.801	3.809	3.805	3.666
	CH ₃	1.308	1.310	1.310	1.300
	RibOH	H-1	3.801	3.799	3.791
	H-1'	3.630	3.637	3.631	3.646
	H-2	3.779	3.787	3.736	3.813
	H-3	3.841	3.848	3.854	3.687
	H-4	4.120	4.112	3.943	3.813
	H-5	4.238	4.233	3.897	3.798
	H-5'	4.110	4.122	3.760	3.646

^aChemical shifts are relative to the signal of DSS (using internal acetone at δ 2.225 p.p.m.) in D₂O. ^bThe primes in structure **4** have been placed to distinguish the "reducing-end" monosaccharides (Gly) from the "non-reducing" ones (Gly').

one cross-peak of Gal H-5 with Gal H-6 and/or H-6', at δ 3.74; an additional cross-peak between H-6 and H-6' is not observed, which indicates that H-6 or H-6' is at a position close to that of H-5 or that those of H-6 and H-6' coincide. However, the cross-peak between Gal H-5 and Gal H-6 and/or H-6' does not show a large geminal coupling for $J_{6,6'}$. Similar features are observed for methyl α -D-galactopyranoside, for which the signals of H-6 and H-6' nearly coincide (Table I). Although the signal for Gal H-5 in **3** is shifted downfield considerably, the nearly identical chemical shifts of the signals for Gal H-6 and H-6' therefore are probably retained in **3**.

It follows that the third signal for an anomeric proton at δ 5.141 comes from

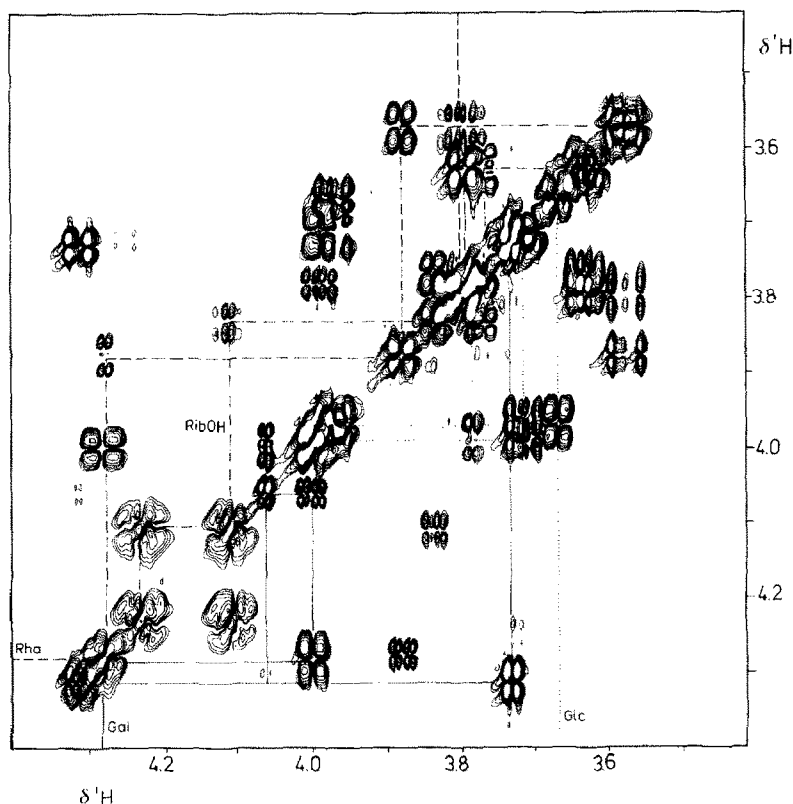


Fig. 2. 500-MHz 2D- ^1H - ^1H Double-quantum-filtered shift-correlation spectrum of **3**. Only the region between 3.5 and 4.3 p.p.m., containing the skeleton-proton resonances, is shown. The lines in the spectrum indicate the spin connectivities for the respective residues.

Glc. Starting from this signal, most of the chemical shifts of the Glc protons (Table I) are obtained from cross-peaks between contiguous protons in the ^1H - ^1H COSY spectrum (Fig. 2). For Glc H-5, only one cross-peak is observed with H-6 and/or H-6', at δ 3.79, whereas the cross-peak between Glc H-6 and H-6' is absent. By the same reasoning as for Gal, it is assumed that Glc H-6 and H-6' both resonate at δ 3.79. A definite assignment of Glc H-6 and H-6', but also of Gal H-6 and H-6', is derived from a ^{13}C - ^1H COSY spectrum, as described below.

For RibOH, all signals are confined to the region of the skeleton protons, but from the difference-spectrum in Fig. 1, the signals for RibOH H-5 and H-5' can be identified at δ 4.238 and 4.110. From this difference-spectrum, $^3J_{\text{POCH}}$ is estimated to be ~ 6.5 Hz for each proton. From the ^{13}C - ^1H COSY spectrum of **3** (see below), it becomes clear that the signal for RibOH H-4 is at δ 4.120, indicating that the signals of RibOH H-4 and H-5' nearly coincide. Therefore, the cross-peak of RibOH at δ 3.841 is the cross-peak between RibOH H-4 and H-3. The signals of the remaining RibOH protons are then assigned from the ^1H - ^1H COSY spectrum (Table I).

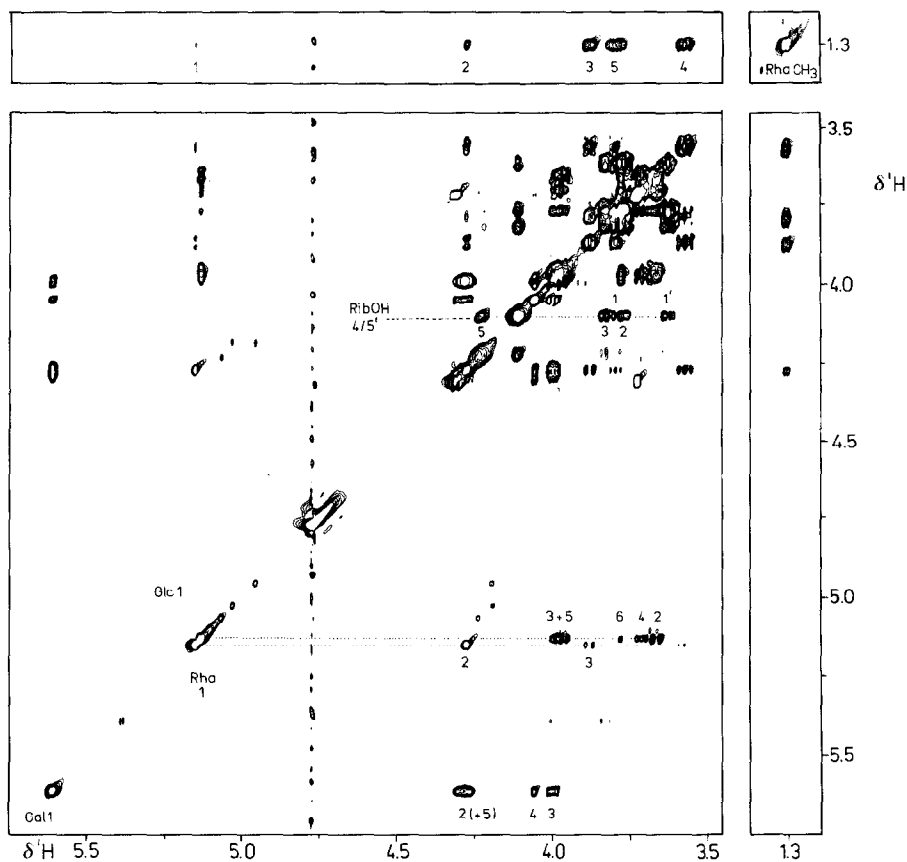


Fig. 3. 500-MHz Homonuclear Hartmann-Hahn spectrum of **3**, with a spin-lock time of 120 ms. For better presentation, the region between 3.3 and 1.9 p.p.m. has been omitted.

For verification of the proton assignments from the ^1H - ^1H COSY spectrum, two HOHAHA experiments were performed with spin-lock times of 80 and 120 ms. In principle, each signal that is part of a scalar coupled network appears as a cross-peak in one cross-section. Starting from the diagonal peak, the magnetisation is transferred from proton to proton *via* this network¹⁴. The rate at which magnetisation is transferred between two coupled protons is proportional to the value of their scalar coupling. The HOHAHA spectrum of **3** with the spin-lock time of 120 ms, shown in Fig. 3, displays more cross-peaks than that obtained with a spin-lock time of 80 ms. For Rha, all signals up to and including that of H-1 are observed in the cross-sections at δ 1.308 for Rha CH_3 , *i.e.*, magnetisation is transferred from CH_3 to H-5, H-4, *etc.*, and to H-1. Starting from Rha H-1 at δ 5.159, only H-2, H-3, and H-4 are observed. The absence of signals for H-5 and CH_3 in the latter cross-sections is due to the small $J_{1,2}$ for Rha. In the cross-sections of the signal for Gal

H-1 at δ 5.623, the signals for Gal H-1,2,3,4 are observed at positions that accord with the assignments from the ^1H - ^1H COSY spectrum. Whether any signal of Gal H-5 is present in these cross-sections is difficult to decide due to overlap with the H-2 signal. No signals for H-6 and H-6' are observed in the cross-section. The cross-sections for the Glc H-1 signal at δ 5.141 show cross-peaks for all protons including signals for H-6 and H-6' at δ 3.79, displaying only small couplings. The appearance of the complete network is in accordance with all contiguous Glc protons having large couplings. For RibOH, all cross-peaks are present in the cross-sections at δ 4.11, the position of the composite signal of RibOH H-4 and H-5'.

When the HOHAHA spectra with spin-locking times of 80 and 120 ms are compared, only a few differences are observed. At 80 ms, the cross-sections for the signals of Rha H-1, Rha CH_3 , Glc H-1, Gal H-1, and RibOH H-4,5' give nearly the same cross-peaks as at 120 ms, *i.e.*, only the signals of the most remote protons in each scalar coupled network are missing. In the cross-sections for the signals of Rha H-1 and CH_3 , these are the signals of H-4 and H-1, respectively. Similarly, the signals of Gal H-5 and RibOH H-1' are absent in the cross-sections for the signals of Gal H-1 and RibOH H-4,5'. Analysis of the cross-peaks of directly coupled protons indicates contributions of dispersive components in a number of cross-peaks¹⁵⁻¹⁸, *e.g.*, Gal H-2,3, Gal H-5,6, and Rha H-3,4.

As mentioned earlier, correlation of ^1H - and ^{13}C -n.m.r. chemical shifts allows

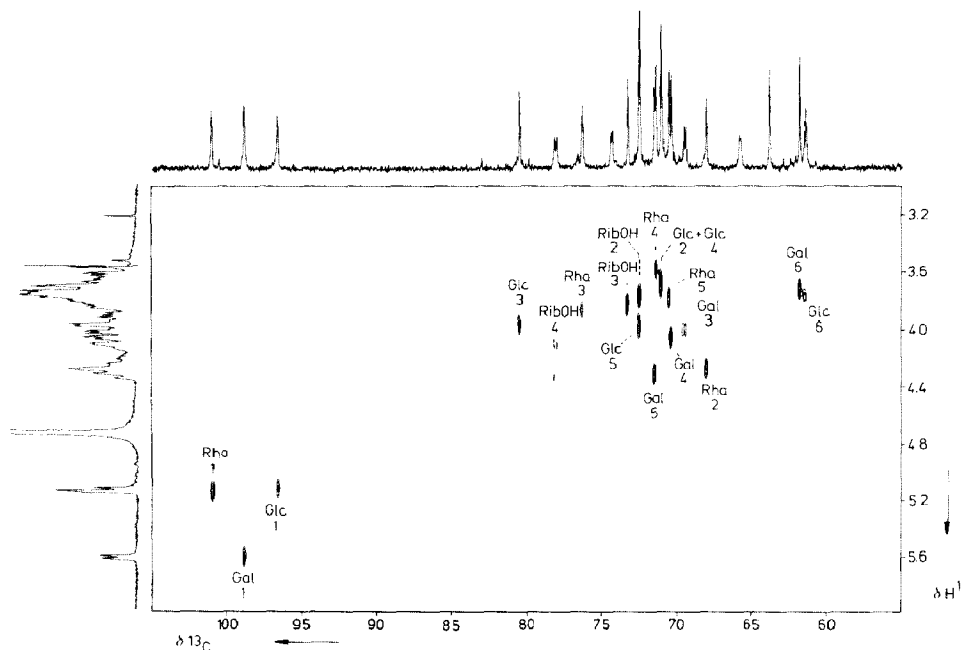


Fig. 4. 2D- ^{13}C - ^1H Heteronuclear shift-correlation spectrum of **3**, at a ^1H -frequency of 200 MHz. To clarify the spectrum, the separate ^1H - and ^{13}C -n.m.r. spectra have been included along the axes of the 2D spectrum.

the identification of the chemical shifts of several protons that are difficult to assign, but *vice versa* the ^{13}C -n.m.r. spectrum may be interpreted using previously determined ^1H -n.m.r. chemical shifts. The ^{13}C -n.m.r. spectrum of **3** is identical to that published for the polymer⁴. The ^{13}C - ^1H COSY spectrum of **3** is presented in Fig. 4. The resolution of the 2D spectrum allows immediate recognition of the majority of the ^{13}C signals. Comparison of the ^{13}C chemical shifts for **3** with those for methyl α -glycopyranosides and RibOH shows downfield shift effects in the signals for **3** for substituted carbons, *i.e.*, for Glc C-3, Rha C-3, and RibOH C-4; upfield shift-effects for the signals of their neighbours accord with the position of the inter-sugar-residue linkages. In the 1D ^{13}C -n.m.r. spectrum, four signals, all in the region between 65–78 p.p.m., have a ^{31}P - ^{13}C coupling and are ascribed to RibOH C-5,

TABLE II

^{13}C -N.M.R. CHEMICAL SHIFT DATA^a (δ) [AND COUPLING CONSTANTS J (Hz)] FOR *Streptococcus pneumoniae* TYPE 6^B CAPSULAR POLYSACCHARIDE **2** AND OLIGOSACCHARIDES **3**, **4**^b, AND **5**, TOGETHER WITH THOSE FOR RIBOH AND THE RESPECTIVE METHYL α -GLYCOPYRANOSIDES OF THE CONSTITUENT MONOSACCHARIDES

Carbon atom	Compound						Methyl α -glyco- pyranosides and RibOH
		2 ^c	3	4		5	
				Gly'	Gly		
Gal	C-1	99.46	98.83 (~1) ^e	100.51	98.77 (~1) ^e	100.57	100.67
	C-2	75.01 (~5)	74.39 (4.8) ^d	69.94	74.36 (6.7) ^d	69.92	69.47
	C-3	70.23 (~6)	69.53 (7.2) ^e	70.65	69.57 (7.0) ^e	70.64	70.76
	C-4	71.14	70.44	70.43	70.43	70.43	70.50
	C-5	72.17	71.56	71.95	71.59	72.00	71.99
	C-6	62.53	61.84	62.10	61.88	62.13	62.50
Glc	C-1	97.19	96.59	96.67	96.73	96.78	100.53
	C-2	71.70	71.09	71.44 ^f	71.36 ^f	71.44	72.51
	C-3	81.25	80.53	80.83 ^h	80.58	80.90 ^h	74.38
	C-4	71.70	71.09	71.05 ^f	71.11 ^f	71.07	72.51
	C-5	73.18	72.52	72.74 ^g	72.55 ^g	72.77	72.86
	C-6	62.21	61.48	61.42	61.42	61.38	61.86
Rha	C-1	101.50	100.96	101.03	101.03	101.06	102.13
	C-2	68.70	68.08	68.15	68.22	68.25	71.55
	C-3	77.03	76.38	76.47	76.62	76.64	71.28
	C-4	72.08	71.44	71.51	71.51	71.51	73.28
	C-5	71.14	70.59	70.65	70.65	70.64	69.68
	C-6	18.61	18.01	18.01	18.01	17.99	17.91
RibOH	C-1	64.50	63.86	63.89	63.84	63.89	63.70
	C-2	73.18	72.52	72.59	72.84	72.85	73.40
	C-3	73.96	73.28	73.30	73.30	73.30	73.51
	C-4	78.75 (~8)	78.14 (7.7) ^e	78.31 (7.4) ^e	79.94 ^h	79.96 ^h	73.40
	C-5	66.49 (~5)	65.84 (3.9) ^d	65.82 (~4) ^d	60.76	60.74	63.70

^aChemical shifts are expressed relative to the signal for acetone at δ 31.55 p.p.m. ^bThe primes in structure **4** have been placed to distinguish the "reducing-end" monosaccharides (Gly) from the "non-reducing" ones (Gly'). ^cRecorded at 40°; coupling constants at 85°, see ref. 4. ^d $J_{^{31}\text{P},^{13}\text{C}}$ Coupling constants. ^e $J_{^{31}\text{P},^{13}\text{C}}$ Coupling constants. ^{f,g,h}Assignments may have to be interchanged.

Gal C-3, Gal C-2, and RibOH C-4. In a ^{13}C - ^1H COSY spectrum, this coupling will be retained as a splitting of the cross-peak in the ^{13}C shift dimension; furthermore, the ^{31}P - ^1H couplings for the signals of Gal H-2 and RibOH H-5 will be retained as well, as a splitting of the cross-peaks in the ^1H shift dimension¹⁹. In the ^{13}C - ^1H COSY spectrum of **3**, only three of these four signals are evident. For two of them, no additional ^{31}P - ^1H coupling is observed in the ^1H frequency domain and these are assigned to Gal C-3 and RibOH C-4. For the third one, ascribed to Gal C-2, the cross-peak with a ^{31}P - ^1H coupling is observed, but only slightly above the noise level of the spectrum and is not included in Fig. 4. RibOH C-5 gives no cross-peak in the 2D spectrum, but the assignment of its signal at δ 65.84, which has ^{31}P - ^{13}C coupling, is obvious. The chemical shift of this signal accords with the resonance position for C-5 of free RibOH with substitution shift effects taken into account (Table II), namely a downfield shift of 4 p.p.m. induced by phosphate substitution¹⁹ partially compensated by a small upfield shift from the Rha substitution at C-4. The hydroxymethyl carbon signal at δ 61.48 gives a cross-peak with the composite signal of Glc H-6 and H-6', and the hydroxymethyl carbon signal at δ 61.84 has a cross-peak with the composite signal of Gal H-6 and H-6'. Consequently, the third hydroxymethyl carbon signal at δ 63.86 belongs to RibOH C-1. The absence of a cross-peak in the 2D spectrum for the latter atom is ascribed to strong proton-proton coupling between RibOH H-2,1,1', together with resolved H-1 and H-1' couplings.

The ^1H -n.m.r. chemical shift data of **3** now allow analysis of a 2D-n.O.e.

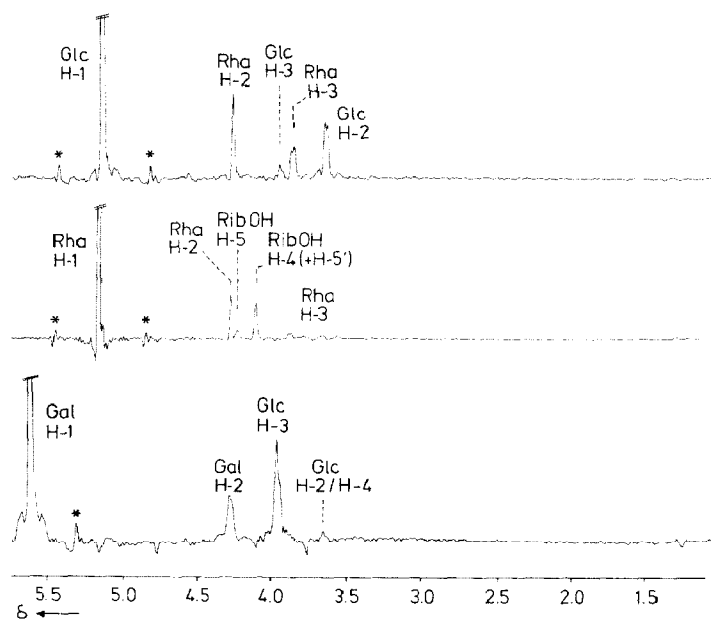


Fig. 5. Added ω_1 -cross-sections of the anomeric protons in the 500-MHz 2D-n.O.e. spectrum of **3**, at a mixing time of 0.5 s. The asterisks denote signals that stem from instrumental imperfections.

spectrum of **3**. The ω_1 -cross-sections for the signals of the anomeric protons in a 500-MHz 2D-n.O.e. spectrum of **3** are presented in Fig. 5. Since the sugar residues in **3** are α , only a limited number of intra-residue n.O.e.-effects are present in these cross-sections, *i.e.*, from Glc H-1 to its H-2 and H-3, from Rha H-1 to its H-2 and H-3, and from Gal H-1 to its H-2. Several inter-residue n.O.e.-effects are observed also, which can be understood when they are compared to the approximate orientation of the respective linkages. From literature data on the conformational analysis by HSEA energy calculations, it can be deduced that α -Gal-(1 \rightarrow 3)-Glc and α -Glc-(1 \rightarrow 3)-Rha linkages have a preferred orientation with ϕ and ψ , the torsion angles that define the orientation of the glycosidic linkage, in the order of -50° and -30° , respectively²⁰. For the α -Gal-(1 \rightarrow 3)-Glc linkage in this orientation, Glc H-3 is by far the nearest interglycosidic proton to Gal H-1; indeed from Gal H-1, the largest inter-residue n.O.e. effect is on Glc H-3. For the α -Glc-(1 \rightarrow 3)-Rha linkage in the preferred orientation, Rha H-2 and H-3 are both equally close to Glc H-1. In the 2D-n.O.e. spectrum, two large interglycosidic n.O.e. effects from Glc H-1 are present on Rha H-2 and H-3. From Rha H-1, inter-residue n.O.e.-effects are on the composite signal of RibOH H-4 and H-5' and on RibOH H-5. As a consequence of the flexibility of the RibOH residue, a conformation around the α -Rha-(1 \rightarrow 4)-RibOH linkage is not easily visualised. However, the exo-anomeric effect²¹ will induce ϕ to be $\sim 60^\circ$, whereby RibOH H-4 and RibOH H-5 and H-5' are at relatively short distance from Rha H-1. The observed n.O.e.-effects are in accord.

(b) *Octasaccharide 4*. The 500-MHz ^1H -n.m.r. spectrum of **4** (Fig. 6) contains six signals for anomeric protons, the positions and coupling constants of which indicate the presence of α sugars. In the difference-spectrum obtained after sub-

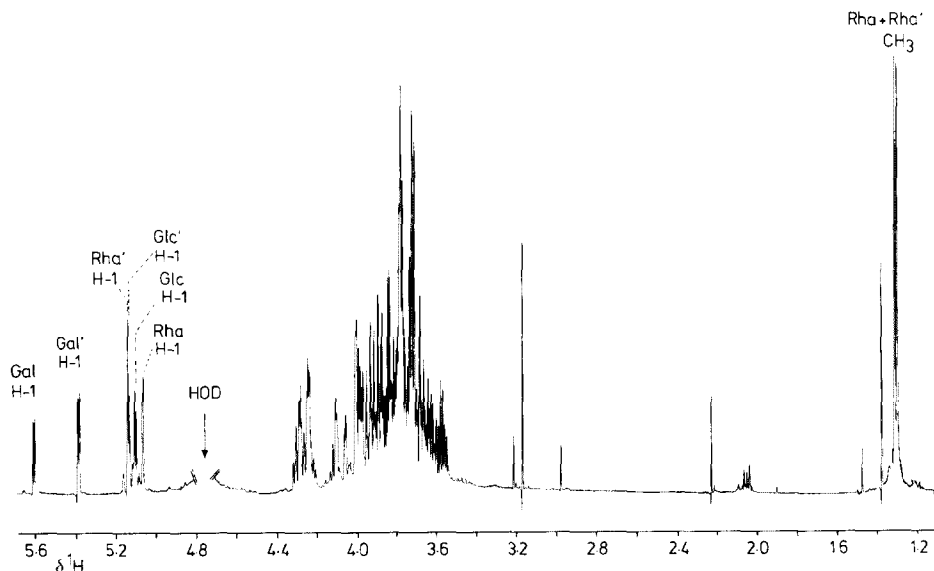


Fig. 6. 500-MHz ^1H -N.m.r. spectrum of **4**.

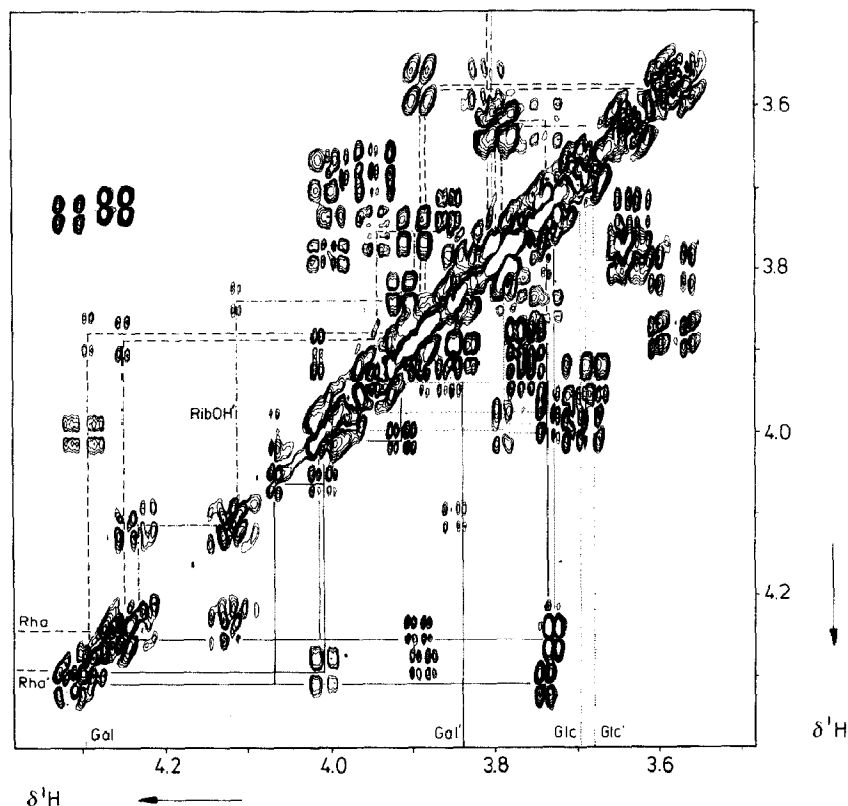


Fig. 7. 500-MHz 2D- ^1H - ^1H Double-quantum-filtered shift-correlation spectrum of **4**. Only the region between 3.5 and 4.3 p.p.m., containing the skeleton-proton resonances, is shown. The lines in the spectrum indicate the spin connectivities for the respective residues.

tracting a 500-MHz ^1H -n.m.r. spectrum of **4** from the corresponding ^{31}P -decoupled spectrum, ^{31}P - ^1H couplings are observed at δ 4.233, 4.122, and 4.295, the positions of the signals of RibOH' H-5,5' and Gal H-2, respectively. The ^{31}P - ^1H coupling constants of these signals are in agreement with those found for **3** (Fig. 1). By combination of the data of the ^1H - ^1H COSY spectrum (Fig. 7), the HOHAHA spectrum with a 120-ms mixing time (data not shown), and the ^1H -n.m.r. chemical shift values for **3**, the ^1H -n.m.r. spectrum of **4** can be assigned completely. For Gal, the ^1H signals in **4** are nearly identical to those of Gal in **3**. The interpretation of the Gal' signals in **4** is obtained as for the corresponding signals in **3**. In the 2D spectrum of **4**, no cross-peak is present between H-4 and H-5 for both Gal and Gal', but the positions of the signals for H-5,6,6' of Gal and Gal' are identified from sets of cross-peaks that have nearly identical appearance and chemical shifts as observed for Gal in **3**. The assignments for the Glc and Glc' residues are based on correlations in the ^1H - ^1H 2D spectra, analogous to those for Glc in **3**. It is not possible to distinguish the Glc and Glc' signals merely from their chemical shifts.

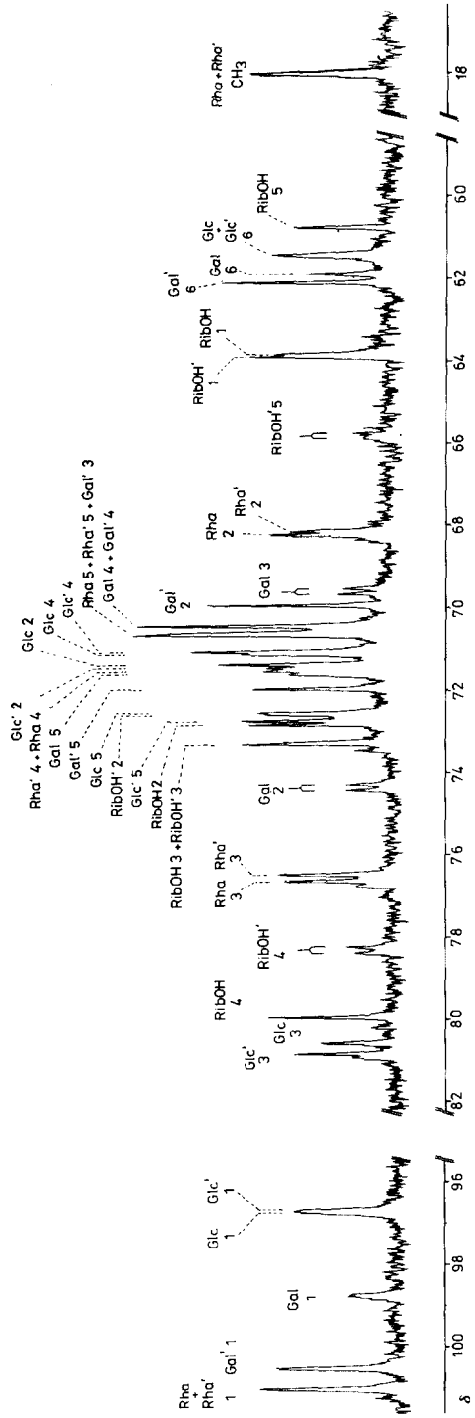


Fig. 8. 50-MHz ¹³C-N.m.r. spectrum of 4.

However, an n.O.e.-effect of Gal H-1 on Glc H-3, present in a 2D-n.O.e. spectrum of **4** (not shown), in combination with significantly differing positions of the signals for Glc H-3 and Glc' H-3, enables the Glc' and Glc signals to be distinguished. The assignments for Rha' in **4** are analogous to those of Rha in **3**. For Rha in **4**, all resonance positions are obtained from the 2D spectra, by comparing the shift positions and the shape of the cross-peaks with those of the other Rha unit. The cross-peaks for RibOH' in the ^1H - ^1H COSY spectrum of **4** are nearly identical to those in **3** (Table I). All signals for RibOH in **4** are in the bulk region of the spectrum and are assigned to the remaining cross-peak resonance positions, using the correlations between these peaks and by comparison to the assignments for **3** and for free RibOH.

The ^1H -n.m.r. chemical shift effects associated with phosphorylation of a sugar residue can be deduced from the data for **4** in Table I. The chemical shifts for the signals of the protons at the phosphate position are downfield from those of the corresponding protons without phosphate, *i.e.*, the signal of Gal H-2 is shifted downfield 0.457 p.p.m. with respect to that of Gal' H-2, and the signals of RibOH' H-5 and H-5' are both at ~ 0.35 p.p.m. to lower field with regard to those of RibOH H-5 and H-5'. The signals of the adjacent protons have also moved downfield, but to a lesser extent (0.10–0.22 p.p.m.). These shift effects accord with those observed for lactose monophosphates¹⁹.

In the ^{13}C -n.m.r. spectrum of **4** (Fig. 8), the signals of Gal and RibOH' are easily identified at positions identical to those of Gal and RibOH in **3**. Also, the ^{31}P - ^{13}C couplings for Gal C-2,3, and RibOH' C-4,5 in **4** have values similar to those for Gal and RibOH in **3**. The ^{13}C -n.m.r. signals of Glc, Glc', Rha, and Rha' in **4** are slightly shifted with regard to the corresponding signals of Glc and Rha in **3**. Analysis of a ^{13}C - ^1H COSY spectrum (data not shown) allows unequivocal assignment of the major part of the ^{13}C -n.m.r. signals of these residues in **4** (Table II). The ^{13}C - ^1H COSY spectrum also affords the chemical shifts of the signals of RibOH: those of C-1,2,3 are at positions close to the signals for C-1,2,3 of RibOH in **3**, but the signals of C-4,5 are shifted due to the absence of phosphate at C-5 of RibOH in **4** (Table II). With the aid of the ^{13}C - ^1H COSY spectrum of **4**, the ^{13}C -n.m.r. signals for Gal' in **4** are found at positions close to those of methyl α -D-galactopyranoside. The signals of several protons of **4** coincide in the ^1H -n.m.r. spectrum, and the signals of the corresponding carbon atoms also have nearly identical chemical shifts. In these instances, the ^{13}C assignments are not certain, as indicated in Table II. For these atoms, the chemical shift values in Table II are interpreted on the basis of closest correspondence to the shift positions for **3** or the methyl α -glycopyranosides.

Table II reflects the ^{13}C -n.m.r. chemical shift effects that occur when phosphate is attached to a sugar residue. In **4**, the signal of Gal C-2 is shifted downfield by 4.42 p.p.m. with respect to that of Gal' C-2, and the signal of RibOH' C-5 is shifted downfield by 5.06 p.p.m. with respect to that of RibOH C-5. Also, the signals of the carbon atoms next to the attachment site, *i.e.*, Gal C-1 and Gal C-3

as well as RibOH' C-4, have shifted upfield by 1.0–1.8 p.p.m. due to the introduction of phosphate. These shift effects accord with ^{13}C -n.m.r. data for lactose monophosphates¹⁹.

As for **3**, the complete list of ^1H -n.m.r. chemical shifts for **4** allows identification of all cross-peaks in a 2D-n.O.e. experiment. Under conditions identical to those for **3**, a large number of cross-peaks are observed, but with lower intensities. All cross-peaks are recognised using the foregoing assignments. The n.O.e.-effects from the anomeric protons are similar for the two repeating units in **4** and for **3**. All inter-residue n.O.e.-effects are analogous to those observed for **3**. The inter-residue n.O.e. from Gal H-1 to Glc H-3 present in this spectrum allows the distinction between the signals for the Glc and Glc' protons for **4**. For compound **4**, no n.O.e.-effects have been recognised, which may be ascribed to an interaction of RibOH' and Gal.

The similar n.O.e. effects for **3** and **4** and the nearly identical n.m.r. data for corresponding partial elements in **3** and **4** suggest identical conformations for these elements. Also, the nearly identical ^{13}C and ^1H chemical shifts for the signals of the phosphate-sugar residues in **3** and **4** indicate that the phosphoric diester linkage in **4** may serve as an adequate model for that linkage in the polymer. The orientation of the two repeating units relative to each other involves four torsion angles across the phosphoric diester linkage. At present, no n.O.e. effects across that linkage can be recognised for **4** and no information is available about the two P–O torsion-angles. Several ^{31}P - ^{13}C and ^{31}P - ^1H couplings have been measured and these contain information about the two phosphoric diester C–O torsion angles. Using modified Karplus equations²², the orientation of the phosphate group relative to Gal in **3** and **4** is inferred from the ^{31}P - ^{13}C and ^{31}P - ^1H coupling constants for this linkage, *i.e.*, $^3J_{\text{POCC-3}} \sim 7$, $^3J_{\text{POCC-1}} \sim 1$, and $^3J_{\text{POCH-2}} \sim 8$ Hz. Three idealised orientations, g^- , g^+ , and *t*, are assumed, with *t* being the orientation wherein the phosphorus atom and H-2 are mutually axial. When the measured coupling constants are regarded as an average of coupling constants for these ideal orientations, the relevant g^- and *t* are populated in a ratio of $\sim 2:1$ ($g^+ < 5\%$), in accordance with previous suggestions⁴. For RibOH in **3** and RibOH' in **4**, only the population can be determined of the orientation for which the phosphate group is *trans* with respect to C-4. From $^3J_{\text{POCH-5}}$ and $^3J_{\text{POCH-5'}}$ (both ~ 6.5 Hz), it can be calculated that the *t* orientation is adopted $\sim 60\%$ of the time.

(c) *Tetrasaccharide 5*. In the 500-MHz ^1H -n.m.r. spectrum of **5**, three signals for α -anomeric protons are present at δ 5.397 (Gal), 5.123 (Glc), and 5.080 (Rha), with shift values and coupling constants corresponding to Gal', Glc, and Rha in **4**, respectively. A doublet at δ 1.314 for CH_3 of Rha is present and the signals of the skeleton protons are all found at δ 4.05–3.55, except for two overlapping signals ascribed to Gal H-5 and Rha H-2 at δ 4.26 (see **4**).

The ^{13}C -n.m.r. spectrum of **5** contains C-1 signals of Gal at δ 100.57, Glc at 96.78, and Rha at 101.06, being assigned by comparison with the signals for **3** and **4**. In a similar way, the Glc C-3, Rha C-3, and RibOH C-4 signals, representing the

linkage positions, are found at δ 80.90, 76.64, and 79.96, respectively. Owing to the absence of phosphorylated RibOH in **5**, the signal for RibOH C-4 appears as a singlet. The remaining signals, as summarised in Table II, have been assigned by reference to the signals for **3** and **4** established by 2D-n.m.r.

From Tables I and II, it is clear that, especially for the ^1H -n.m.r. data, large chemical shift deviations occur relative to the monosaccharides. These shift effects are not accounted for by simple addition of substituent effects, and are probably more complex due to unknown conformational aspects.

Recently²³, several new 2D-n.m.r. techniques were applied for the complete ^1H - and ^{13}C -n.m.r. assignment of a capsular polysaccharide containing one phosphate and two sugar residues per repeating unit. In that investigation, ^1H -detected ^{13}C - ^1H COSY techniques were applied on a 500-MHz spectrometer, leading to a large reduction in measuring time as compared to our methods. The present heteronuclear spectra were recorded in ~ 60 h on a 200-MHz spectrometer, giving a reasonable signal-to-noise ratio. However, on a 500-MHz n.m.r. spectrometer, a considerable reduction of measuring time should be obtainable. This renders the ^{13}C -detected ^{13}C - ^1H COSY experiment, with ^1H decoupling in t_1 , still highly competitive to the ^1H -detected variant.

EXPERIMENTAL

Streptococcus pneumoniae serotype 6^B (Statens Seruminstitut, Copenhagen, Denmark) was grown on Worfel Ferguson agar (Difco Laboratories) and the capsular polysaccharide was isolated by conventional ethanol-precipitation procedures. In order to remove contaminating mannan, the crude polysaccharide (500 mg) was passed twice over a Concanavalin-A affinity column (3×30 cm), using a buffer containing 0.1M NaOAc, 0.15M NaCl, mM MgCl_2 , mM MnCl_2 , and mM CaCl_2 (pH 6.5), dialysed for 48 h against demineralised water, and lyophilised.

Alkaline hydrolysis. — Polysaccharide **2** (100 mg) was hydrolysed with 10mM NaOH (20 mL) for 72 h at 85°. After neutralisation with M HCl, the hydrolysate was fractionated on a column (40×3 cm) of Bio-Gel P2 (Bio Rad), using twice-distilled water as eluent and refractive index monitoring (Bischoff-differential refractometer LCD 202). The fractions were analysed for carbohydrate by t.l.c. on Silica Gel 60 F₂₅₄ (Merck), using 6:5:5 1-butanol-pyridine-water and detection with orcinol-sulfuric acid. Incompletely hydrolysed polysaccharide fractions were resubmitted to alkaline hydrolysis. Combined oligosaccharide fractions were separated on a column (145×2 cm) of Bio-Gel P6 (Bio Rad), using 50mM NH_4HCO_3 buffer (pH 8.0), monitored by u.v. detection at 214 nm (LKB 2238 Uvicord S II) and orcinol-sulfuric acid, yielding **3** (39 mg) as the major product.

Acid hydrolysis. — Partial hydrolysis with hydrogen fluoride was performed on **2** (50 mg) in two ways. *Method I.* Polysaccharide **2** (50 mg) was incubated with aqueous 48% HF (3 mL) in a plastic vial at 4° for 48 h. After evaporation of the HF in a desiccator (~ 15 mmHg) over KOH and subsequent gel-filtration on Bio-

Gel P2 and P6, fractions were obtained with **4** (6 mg) and **5** (12 mg) as the major products. *Method II.* Polysaccharide **2** (50 mg) was incubated with aqueous 48% HF (3 mL) in a plastic vial at -16° for 4 days⁴. The reaction mixture was concentrated in a desiccator (~ 1 mmHg) over KOH, and a solution of the residue in water (10 mL) was neutralised with aqueous 25% ammonia. The oligosaccharides were purified by subsequent gel-filtrations as described above, yielding **4** as the major product (19 mg). The two minor fractions (5 mg each) eluted first from P6 had R_F values in t.l.c. lower than that of **4**, indicating the presence of higher oligomers.

Analytical methods. — Sugar analysis was carried out by g.l.c. on a CP-Sil 5 WCOT fused-silica capillary column (25 m \times 0.32 mm i.d.), using a Varian Aerograph 3700 gas chromatograph^{24,25}.

G.l.c.-(e.i.)m.s. was performed on a Carlo Erba GC/Kratos MS80/Kratos DS 55 system (electron energy, 70 eV; accelerating voltage, 2.7 kV; ionising current, 100 μ A; ion-source temperature, 225 $^{\circ}$; BP-1 capillary column). Negative- and positive-ion f.a.b.-mass spectra were recorded on a VG Analytical ZAB-HF mass spectrometer (Xe-beam, 7.6 keV; acceleration voltage, 8 kV). The carbohydrate samples were dissolved or dispersed in a glycerol matrix. Linear mass scans over 1500 daltons were recorded with an u.v. chart recorder (Department of Mass Spectrometry, Utrecht University).

500-MHz ^1H -n.m.r. spectra were recorded at 27 $^{\circ}$ with a Bruker AM-500 spectrometer controlled by an Aspect 3000 computer (Department of NMR Spectroscopy, Utrecht University, and SON-hf-NMR facility, Department of Biophysical Chemistry, Nijmegen University). Prior to ^1H -n.m.r. spectroscopy, the samples were repeatedly exchanged in D_2O with intermediate lyophilisation. Finally, the material was dissolved in 0.4 mL of D_2O (99.96% atom D). In each n.m.r. experiment, ~ 12 g of material was used and the measurements were performed in D_2O at pD 4.5 for **3** and pD 6.5 for **4** and **5**. For the 2D-n.O.e. experiment on **4**, the pD was adjusted to 4.5. Chemical shifts (δ) are expressed in p.p.m. downfield from internal sodium 4,4-dimethyl-4-silapentane-1-sulphonate (DSS), but were actually measured by reference to internal acetone (δ 2.225 in D_2O at 27 $^{\circ}$). Resolution-enhancement of the spectra was achieved by Lorentzian-to-Gaussian transformation.

^{31}P -Decoupling in the ^1H -n.m.r. spectrum was achieved by an external source with inbuilt phase-cycling necessary for Waltz-decoupling²⁶. A broad-band probe, tuned for ^1H and ^{31}P , was used to record this spectrum.

^1H - ^1H Shift-correlation (COSY) spectra were recorded by a three-pulse sequence, $90^{\circ}-t_1-90^{\circ}-90^{\circ}$ -acq, where phase-cycling of the receiver and detector allowed for coherence transfer through a double quantum filter²⁷. A $600 \times 2\text{k}$ data matrix was obtained with 32 scans for each experiment and was zero-filled to $2\text{k} \times 4\text{k}$, prior to Fourier-transformation. Resolution enhancement in ω_2 and suppression of truncation artifacts in ω_1 were obtained by a $\pi/4$ -shifted sine-squared bell function in t_2 and a cosine-squared bell function in t_1 . In order to suppress double quantum coherence transfer between consecutive scans, the relaxation delay was varied randomly²⁸ between 0.6 and 0.8 s.

Homonuclear Hartmann–Hahn (HOHAHA) spin-lock experiments^{14,15,29} were performed using the pulse-sequence $90^\circ-t_1$ -SL-acq, wherein SL stands for a multiple of the MLEV-17 sequence²⁹ preceded and followed by a 1-ms spin-lock pulse. The spin-lock field-strength corresponded to a 90° pulse-width of $25\ \mu\text{s}$ and the total spin-lock mixing time was 80 or 120 ms. A data-matrix of $600 \times 2\text{k}$ was obtained, with 16 scans for each experiment, and, prior to Fourier transformation, the matrix was zero-filled to $2\text{k} \times 4\text{k}$. For resolution-enhancement, a $\pi/4$ -shifted sine-squared bell function was applied in each time domain.

In the 2D-n.O.e. experiment^{30,31}, the mixing period was arbitrarily set to 0.5 s. Axial peaks and coherent components, with the exception of zero-quantum coherencies, were eliminated by appropriate cycling of detection-pulse-phase and receiver-phase^{30,31}. A data matrix was obtained of $680 \times 4\text{k}$ points, which was zero-filled to $2\text{k} \times 4\text{k}$ prior to Fourier transformation. For resolution-enhancement and suppression of truncation artifacts, a $\pi/4$ -shifted sine-squared bell function was applied in each dimension. For analysis of the n.O.e. effects, a number of ω_1 cross-sections of a specific signal were added. Compared to a single cross-section, this improved the signal-to-noise ratio. When the signals from cross-relaxation are phase-adjusted to be absorptive, zero-quantum contributions to cross-peaks will be dispersive, rendering a net zero intensity³². Consequently, co-addition of all cross-sections from a specific signal will result in suppression of the afore-mentioned zero-quantum contributions.

All 2D- ^1H - ^1H experiments were performed at 27° , except the 2D-n.O.e. experiment with **4**, which was carried out at 10° . In each experiment, the residual HDO signal was saturated during the recycle-delay. Also TPPI was applied in each experiment to make a phase-sensitive handling in ω_1 possible³³. The spectral width was set to 2500 Hz, which meant an increment for t_1 of 0.2 ms for the consecutive spectra in the 2D- ^1H - ^1H experiments.

The 50-MHz ^{13}C -n.m.r. experiments were performed at 27° on a Bruker WM-200 spectrometer equipped with a 5-mm broad-band probe head, operating in the pulsed F.t. mode and controlled by an Aspect 2000 computer (SON-hf-NMR-facility, Department of Biophysical Chemistry, Nijmegen University, The Netherlands). ^{13}C -N.m.r. chemical shifts (δ) are expressed in p.p.m. relative to internal acetone at δ 31.55, with an accuracy of ± 0.02 p.p.m. The 2D- ^{13}C - ^1H COSY experiments were performed with simultaneous suppression of ^1H homonuclear couplings^{34,35} using the standard Bruker pulse program XHCORRD, with the phase-cycling of the refocussing pulse as described³⁶. Refocussing delays as required in the experiment were adjusted to an average $^1J_{\text{C,H}}$ coupling constant of 150 Hz³⁷. ^1H and ^{13}C 90° pulse-widths were 8 and $12\ \mu\text{s}$, respectively. Pulse-widths for ^1H were determined as described³⁷. A $96 \times 4\text{k}$ data matrix was acquired, which was zero-filled prior to Fourier transformation to obtain a $2\text{k} \times 8\text{k}$ spectral data matrix. A $\pi/4$ -shifted sine-squared function for ^{13}C -subspectra and a non-shifted sine-bell function for ^1H -subspectra were applied to enhance resolution.

ACKNOWLEDGMENTS

We thank Mr. Rien de Reuver for growing the bacteria, Mrs. Anca van der Kerk-van Hoof and Mr. Cees Versluis for recording the mass spectra, and Centra-science B.V., Etten-Leur (The Netherlands) and the Netherlands Organization for Scientific Research (SON/NWO) for financial support.

REFERENCES

- 1 H. SNIPPE, J. E. G. VAN DAM, A. J. VAN HOUTE, J. M. N. WILLERS, J. P. KAMERLING, AND J. F. G. VLIAGENTHART, *Infect. Immun.*, 42 (1983) 842-844.
- 2 F. KAUFMANN, E. LUND, AND B. E. EDDY, *Int. Bull. Bacteriol. Nomencl. Taxon.*, 10 (1960) 30-41.
- 3 P. A. REBERS AND M. HEIDELBERGER, *J. Am. Chem. Soc.*, 83 (1961) 3056-3059.
- 4 L. KENNE, B. LINDBERG, AND J. K. MADDEN, *Carbohydr. Res.*, 73 (1979) 175-182.
- 5 G. ZON, S. C. SZU, W. EGAN, J. D. ROBBINS, AND J. B. ROBBINS, *Infect. Immun.*, 37 (1982) 89-103.
- 6 J. G. HOWARD, H. ZOLA, G. H. CRISTIE, AND B. M. COURTENAY, *Immunology*, 21 (1971) 535-546.
- 7 W.H.O. Expert Committee on Biological Standardization, 28th Report, *W.H.O. Rep. Ser.*, 610 (1977) 1-33.
- 8 J. B. ROBBINS, R. AUSTRIAN, C.-J. LEE, S. C. RASTOGI, G. SCHIFFMAN, J. HENRICHSEN, P. H. MÄKELÄ, C. V. BROOME, R. R. FACKLAM, R. H. TIESJEMA, AND J. C. PARKE, *J. Infect. Dis.*, 148 (1983) 1136-1159.
- 9 M. PORRO, P. COSTANTINO, S. VITI, F. VANNOZZI, A. NAGGI, AND G. TORRI, *Mol. Immunol.*, 22 (1985) 907-919.
- 10 M. IKAWA, J. W. MORROW, AND S. J. HARNEY, *J. Bacteriol.*, 92 (1966) 812-814.
- 11 A. R. ARCHIBALD AND J. BADDILEY, *Adv. Carbohydr. Chem.*, 21 (1966) 323-375.
- 12 J. P. KAMERLING, W. HEERMA, J. F. G. VLIAGENTHART, B. N. GREEN, I. A. S. LEWIS, G. STRECKER, AND G. SPIK, *Biomed. Mass Spectrom.*, 10 (1983) 420-425.
- 13 A. DELL AND C. E. BALLOU, *Biomed. Mass Spectrom.*, 10 (1983) 50-56.
- 14 D. G. DAVIS AND A. BAX, *J. Am. Chem. Soc.*, 107 (1985) 2820-2821.
- 15 L. BRAUNSCHWEILER AND R. R. ERNST, *J. Magn. Reson.*, 53 (1983) 521-528.
- 16 A. BAX AND D. G. DAVIS, in N. NICOLAI AND G. VALENSIN (Eds.), *Advanced Magnetic Resonance Techniques in Systems of High Molecular Complexity*, Birkhauser, Basel, 1986, and references therein.
- 17 L. MÜLLER AND R. R. ERNST, *Mol. Phys.*, 38 (1979) 963-992.
- 18 G. C. CHINGAS, A. N. GARROWAY, R. D. BERTRAND, AND W. B. MONIZ, *J. Chem. Phys.*, 74 (1981) 127-156.
- 19 J. BREG, D. ROMIJN, H. VAN HALBEEK, J. F. G. VLIAGENTHART, R. A. VISSER, AND C. A. G. HAASNOOT, *Carbohydr. Res.*, 174 (1988) 23-36.
- 20 K. BOCK, A. BRIGNOLE, AND B. W. SIGURSKJOLD, *J. Chem. Soc., Perkin Trans. 2*, (1986) 1711-1713.
- 21 R. U. LEMIEUX, K. BOCK, L. T. J. DELBAERE, S. KOTO, AND V. RAO, *Can. J. Chem.*, 58 (1980) 631-653.
- 22 P. P. LANKHORST, C. A. G. HAASNOOT, C. ERKELENS, AND C. ALTONA, *J. Biomol. Struct. Dyn.*, 1 (1984) 1387-1405.
- 23 R. A. BYRD, W. EGAN, M. F. SUMMERS, AND A. BAX, *Carbohydr. Res.*, 166 (1987) 47-58.
- 24 J. P. KAMERLING AND J. F. G. VLIAGENTHART, *Cell Biol. Monogr.*, 10 (1982) 95-125.
- 25 G. J. GERWIG, J. P. KAMERLING, AND J. F. G. VLIAGENTHART, *Carbohydr. Res.*, 129 (1984) 149-157.
- 26 A. J. SHAKA, J. KEELER, AND R. FREEMAN, *J. Magn. Reson.*, 53 (1983) 313-340.
- 27 M. RANCE, O. W. SØRENSEN, G. BODENHAUSEN, G. WAGNER, R. R. ERNST, AND K. WÜTHRICH, *Biochem. Biophys. Res. Commun.*, 117 (1983) 479-485.
- 28 J. A. W. H. VERMEULEN, R. M. J. N. LAMERICHS, A. DE MARCO, M. LLIN'AS, R. BOELENS, J. ALLEMAN, AND R. KAPTEIN, *FEBS Lett.*, 219 (1987) 426-430.
- 29 A. BAX AND D. G. DAVIS, *J. Magn. Reson.*, 65 (1985) 355-360.
- 30 S. MACURA AND R. R. ERNST, *Mol. Phys.*, 41 (1980) 95-117.
- 31 A. KUMAR, R. R. ERNST, AND K. WÜTHRICH, *Biochem. Biophys. Res. Commun.*, 95 (1980) 1-6.
- 32 S. MACURA, Y. HUANG, D. SUTER, AND R. R. ERNST, *J. Magn. Reson.*, 43 (1981) 259-281.

- 33 D. MARION AND K. WÜTHRICH, *Biochem. Biophys. Res. Commun.*, 117 (1983) 967-974.
- 34 A. BAX, *J. Magn. Reson.*, 53 (1983) 517-520.
- 35 V. RUTAR, *J. Magn. Reson.*, 58 (1984) 306-310.
- 36 J. A. WILDE AND P. H. BOLTON, *J. Magn. Reson.*, 59 (1984) 343-346.
- 37 L. D. HALL AND G. A. MORRIS, *Carbohydr. Res.*, 82 (1980) 175-184.